0013-7227/06/$15.00/0
Printed in U.S.A.

Endocrinology 147(7):3398–3407

doi: 10.1210/en.2005-1494

Chronic Palmitate But Not Oleate Exposure Induces Endoplasmic Reticulum Stress, Which May Contribute to INS-1 Pancreatic β-Cell Apoptosis

Elizabeth Karaskov, Cameron Scott, Liling Zhang, Tracy Teodoro, Mariella Ravazzola, and Allen Volchuk

Division of Cell and Molecular Biology (E.K., L.Z., T.T., A.V.), Toronto General Research Institute, University Health Network, MBRC 4R402 Toronto, Ontario, Canada M5G 2C4; Department of Biochemistry (C.S., A.V.), University of Toronto, Toronto, Ontario, Canada M5S 1A8; Department of Cell Physiology and Metabolism (M.R.), University of Geneva Medical Center, 1211 Geneva 4, Switzerland

Chronic free fatty acid (FFA) exposure induces pancreatic β-cell death, which may contribute to the development of type 2 diabetes. The mechanisms involved in FFA-induced cell death are not completely understood. Here we have investigated the effect of FFA on endoplasmic reticulum (ER) stress pathways in INS-1 pancreatic β-cells. INS-1 cells exposed to palmitate for 16–24 h under serum-free conditions showed marked apoptosis and increased protein levels of phosphorylated eukaryotic translation initiation factor 2α (eIF2α), activating transcription factor 4 (ATF4), X box-binding protein 1 (XBP-1), and C/EBP homologous transcription factor (CHOP) compared with control cells. The CHOP transcription factor has been implicated in mediating ER stress-induced apoptosis. Unexpectedly, the levels of the ER chaperone proteins Grp78/BiP and PDI were not affected by palmitate treatment, suggesting that the cell protective aspects of the unfolded protein response (UPR) are not up-regulated by palmitate. Palmitate-treated cells had markedly altered distribution of ER chaperones and altered ER morphology, suggesting that accumulation of misfolded proteins might trigger the ER stress response. In contrast, oleate treatment did not significantly induce the UPR pathways, nor was it as detrimental to INS-1 β-cells. The results suggest that activation of the UPR may significantly contribute to palmitate- but not oleate-induced pancreatic β-cell death. (*Endocrinology* 147: 3398–3407, 2006)

DEVELOPMENT OF TYPE 2 diabetes occurs when pancreatic β-cells are unable to compensate for insulin resistance in peripheral tissues (1). This is particularly relevant in obese individuals who are commonly insulin resistant. Pancreatic β-cells fail to compensate for insulin resistance because of defects in insulin secretion or loss of β-cell mass because of cell death (2). The underlying causes of β-cell death are beginning to be uncovered. Inflammatory cytokines such as TNFα, IL-1β, and interferon-γ have been shown to be cytotoxic to β-cells (3) and may contribute to β-cell death in obesity, which has been described as a state of low-level chronic inflammation (4). Lipotoxicity has also emerged as a potential contributor to β-cell decompensation (5–8). Nonesterified free fatty acids (FFA) have been shown to be cytotoxic to β-cells in obesity-associated diabetes models as well as in normal β-cells from several species (9–14).

Although it is believed that lipotoxicity occurs as a result of excess FFA that enter nonoxidative metabolic pathways, the molecular mechanism by which FFA cause β-cell death is not completely understood. In the obese diabetic Zucker fatty rat model, excess FFA cause elevated ceramide levels, leading to increased amounts of the inducible isoform of nitric oxide synthase and nitric oxide (NO) generation, which can trigger β-cell apoptosis (13–15). However, several studies have failed to implicate NO involvement in FFA-induced β-cell death (9, 12, 16). In addition, FFA can be cytotoxic by inducing apoptotic pathways that originate as a result of mitochondrial perturbation and increased oxidative stress (9, 12, 17).

A recent study by Ozcan *et al.* (18) has uncovered a link between obesity and endoplasmic reticulum (ER) stress in liver and adipose cells. The ER is involved in folding, processing, and export of newly synthesized secretory and membrane proteins. An increase in the amount of proteins requiring folding or alterations in the ER environment that decreases folding capacity can elicit the unfolded protein response (UPR), a mechanism that counteracts ER stress (19, 20). When counterregulatory mechanisms such as transient inhibition of protein synthesis, elevated ER chaperone levels, and ER-associated degradation components cannot compensate for the imposed ER stress, cell death pathways are initiated. Pancreatic β-cells are particularly sensitive to ER stress because these cells must synthesize and secrete large amounts of insulin to meet metabolic demands (21, 22).

Given the link between hepatic and fat cell ER stress and obesity, we examined the effects of chronic FFA treatment on UPR signaling in the INS-1 cell culture model of pancreatic β-cells. We found that although chronic treatment with either

First Published Online April 6, 2006

Abbreviations: ATF4, Activating transcription factor 4; BiP, Ig heavy chain-binding protein; CHOP, C/EBP homologous transcription factor; eIF2α, eukaryotic translation initiation factor 2α; ER, endoplasmic reticulum; FBS, fetal bovine serum; FFA, free fatty acids; GADD153, growth arrest and DNA damage-inducible protein; Grp78, glucose-regulated protein 78 kDa; HA, hemagglutinin; IRE1, inositol-requiring enzyme 1; PDI, protein disulfide isomerase; PERK, PKR-like ER kinase; PMSF, phenylmethylsulfonyl fluoride; UPR, unfolded protein response; XBP-1, X box-binding protein 1.

***Endocrinology* is published monthly by The Endocrine Society (http://www.endo-society.org), the foremost professional society serving the endocrine community.**

palmitate or oleate was cytotoxic, only palmitate induced significant ER stress.

Materials and Methods

Antibodies

Phosphorylated eukaryotic translation initiation factor 2α (phospho-eIF2α) (Cell Signaling, Beverly, MA; no. 9721, 1:500), eIF2α (Cell Signaling; no. 9722, 1:500), phosho-PKR-like ER kinase (PERK) (Cell Signaling, no. 3191, 1:500), cAMP response element-binding protein 2/activating transcription factor 4 (ATF4) (Santa Cruz; sc-200, 1:500), growth arrest and DNA damage-inducible protein (GADD153)/C/EBP homologous transcription factor (CHOP) (Santa Cruz; sc-575, 1:500), X box-binding protein 1 (XBP-1) (Santa Cruz; sc-7160, 1:500), anti-KDEL (StressGen Biotechnology, Victoria, Canada; SPA-827, 1:1000), protein disulfide isomerase (PDI) (StressGen; SPA-890, 1:4000), γ-tubulin (Sigma Chemical Co., St. Louis, MO; T6557, 1:1000), monoclonal antihemagglutinin (anti-HA) (HA.11; Babco Inc., Richmond, CA). A rabbit polyclonal antibody to glucose-regulated protein 78 kDa (Grp78)/Ig heavy chain-binding protein (BiP) was kindly provided by Dr. Ingrid Haas (Max-Planck Institute, Freiberg, Germany).

INS-1 cell culture

Rat INS-1 pancreatic β-cells were maintained in RPMI 1640 (11 mM glucose, 1 mM sodium pyruvate, 10 mM HEPES) supplemented with 10% fetal bovine serum (FBS), 2 mM L-glutamine, and 55 μM β-mercaptoethanol at 37 C/5% CO_2. During FFA stimulation, the above medium was used but in the absence of FBS. All experiments were performed between passages P4 and P20.

FFA preparation, cell treatment, and lyses

FFA solutions were prepared as described previously (23). Briefly, 100 mM palmitate (Sigma no. P-0500) and 100 mM oleate (Sigma no. O-7501) stocks were prepared in 0.1 M NaOH at 70 C and filtered. Five percent (wt/vol) FFA-free BSA (Sigma no. A-6003) solution was prepared in double-distilled H_2O and filtered. A 5 mM FFA/5% BSA solution was prepared by complexing an appropriate amount of FFA to 5% BSA in a 60 C water bath. The above solution was then cooled to room temperature and diluted 1:5 in RPMI 1640 without FBS to a final concentration of 1 mM FFA/1% BSA.

INS-1 cells were cultured on 10-cm dishes to 80–85% confluency and stimulated with 1 mM FFA/1% BSA for 3, 6, 16, and 24 h. One micromolar thapsigargin (1 and 6 h) and 2 μg/ml tunicamycin (16 h) were used as positive controls for induction of ER stress. At indicated time points, the cells were washed in PBS and lysed in ice-cold lysis buffer [1% Triton X-100, 20 mM HEPES (pH 7.4), 100 mM KCl, 2 mM EDTA, 1 mM phenylmethylsulfonyl fluoride (PMSF), 10 μg/ml leupeptin, 10 μg/ml aprotinin, 10 mM NaF, 2 mM Na_3VO_4, and 10 nM okadaic acid]. The cells were lysed on ice for 30–60 min and centrifuged at 13,000 rpm for 10 min at 4 C. The supernatant was then transferred to a new tube, and protein concentration was determined with BCA reagent (Pierce Chemical Co., Rockford, IL; no. 23223).

Cell transfection

INS-1 cells (400,000 cells per well) were seeded onto glass coverslips in 24-well dishes the day before transfection. Cell were transfected with HA-ATF6 plasmid pCGN-ATF6 (obtained from Dr. Ron Pyrews, Columbia University, New York, NY) using Lipofectamine 2000 reagent (Invitrogen, Carlsbad, CA) according to the manufacturer's suggested protocol. Sixteen to 24 h later, the cells were treated as described in the Fig. 6 legend and processed for indirect immunofluorescence microscopy as described below.

Preparation of nuclear extracts

INS-1 cells were treated with FFA or controls as described above. At 6 and 16 h, the cells were washed in PBS and lysed in ice-cold nuclear extraction buffer A [10 mM HEPES (pH 7.5), 10 mM KCl, 1.5 mM $MgCl_2$, 0.1 mM PMSF, 10 μg/ml leupeptin, 10 μg/ml aprotinin, and 1 mM dithiothreitol (DTT)]. The samples were incubated on ice for 30 min, homogenized by passing through 25-gauge needle 10 times, and centrifuged at 13,000 rpm for 30 sec at 4 C to pellet nuclei. The pellet was resuspended in nuclear extraction buffer C [20 mM HEPES (pH 7.9), 10% glycerol, 400 mM NaCl, 40 mM $MgCl_2$, 1 mM EDTA, 0.1 mM PMSF, 10 μg/ml leupeptin, 10 μg/ml aprotinin, and 1 mM DTT] and incubated on ice for 30 min. The samples were then centrifuged at 13,000 rpm for 15 min at 4 C. Nuclear extracts were resolved on SDS-PAGE, transferred to nitrocellulose, and immunoblotted with anti-ATF4 antibody.

Apoptosis assay

The cell death detection kit ELISA^{PLUS} (Roche Diagnostics, Indianapolis, IN) was used to monitor FFA-induced apoptosis. One day before the experiments, INS-1 cells were seeded in 24-well plates (200,000 cells per well). The cells were treated as indicated in the Fig. 1 legend. After the treatment, the cells were lysed and oligonucleosomes in the cytoplasm quantified according to the manufacturer's instructions. Cytoplasmic oligonucleosomes are indicative of apoptosis-associated DNA degradation. Cells grown in the presence of serum had near background levels of cytoplasmic oligonucleosomes, and consequently all other treatment conditions were normalized to this condition at each time point.

Immunofluorescence microscopy

INS-1 cells were seeded on glass coverslips in 24-well dishes. After an overnight incubation, the cells were treated as indicated in the legends to Figs. 5 and 6. After the treatments, the cells were washed twice with PBS and fixed for 20 min in 4% paraformaldehyde/PBS at room temperature. The cells were subsequently washed twice in PBS and incubated in blocking solution for 1 h (2% nonfat milk/2% BSA in PBS). Primary antibodies were added for 1 h at room temperature in blocking solution [mouse anti-KDEL (1:200) or mouse anti-HA (1:1000)]. After three washes (5 min each) in PBS, Oregon green-labeled antimouse secondary (Molecular Probes, Inc., Eugene, OR) was added for 1 h at room temperature. The cells were washed three times (5 min each) and mounted onto glass slides using Fluoromount G mounting medium (Electron Microscopy Sciences, Inc., Hatfield, PA). Confocal images were acquired using a Zeiss laser scanning confocal microscope (Carl Zeiss, Inc., Thornwood, NY).

Electron microscopy

INS-1 cells were fixed with 2% glutaraldehyde in 0.15 M sodium phosphate buffer (pH 7.4) for 30 min at room temperature. The samples were postfixed in 2% OsO_4, contrasted by en bloc staining with uranyl acetate (24), dehydrated with alcohol, and embedded in Epon. For immunoelectron microscopy, cells were fixed as above and processed for cryo-ultramicrotomy as described (25). Ultrathin frozen sections were prepared and incubated for immunolabeling as described (26). Monoclonal anti-Grp78/BiP antibody (StressGen) was diluted 1:50 and was labeled with goat antimouse IgG gold (gold size, 10 nm).

^{35}S labeling and immunoprecipitation

One million INS-1 cells per well were plated in a six-well dish the day before the start of the experiment. The cells were treated with 1 mM FFA/1% BSA (prepared in L-methionine-free RPMI 1640) or 2 μg/ml tunicamycin, in the presence of 100 μCi/ml of Tran^{35}S-Label (MP Biomedicals, Irvine, CA; no. 51006) for 3, 6, and 9 h at 37 C. At the indicated time points, the cells were washed in PBS and lysed in ice-cold lysis buffer [1% Triton X-100, 20 mM HEPES (pH 7.4), 100 mM KCl, 2 mM EDTA, 1 mM DTT, 1 mM PMSF, 10 μg/ml leupeptin, and 10 μg/ml aprotinin] for 1 h at 4 C. The lysates were then centrifuged at 13,000 rpm for 10 min at 4 C, and 150 μg of the cleared lysate, as determined by BCA assay, was used for immunoprecipitation with rabbit polyclonal Grp78/BiP antibody at 4 C overnight. The next day, protein A-agarose was added (25 μl/immunoprecipitation), and incubation continued for another 2 h at 4 C. The unbound fraction was removed and the pellet was washed four times with 1 ml lysis buffer for 5 min at 4 C. The pellet was resuspended directly in Laemmli sample buffer and protein resolved by SDS-PAGE. The dried gel was exposed overnight in a Molecular Dy-

namics phosphor screen, which was scanned using a PhosphorImager (Molecular Dynamics, Sunnyvale, CA) and quantified using ImageQuant software.

[^{3}H]Leucine incorporation into total cellular protein

INS-1 cells (500,000 cells per well) were seeded in 12-well dishes. Forty-eight hours later, the cells were washed in PBS and treated as follows: 1% BSA, 1 mM palmitate/1%BSA, 1 mM oleate/1%BSA, or thapsigargin (1 μM), all in serum-free media containing 25 μCi/ml [^{3}H]leucine (PerkinElmer, Boston, MA). After treatment for 3, 6, and 9 h, the cells were placed on ice. The cells were washed twice with ice-cold PBS and lysed in 1% Triton X-100, 20 mM HEPES (pH 7.4), 100 mM KCl, 2 mM EDTA, 1 mM DTT, 1 mM PMSF, 10 μg/ml leupeptin, and 10 μg/ml aprotinin. Total protein from each condition was precipitated with trichloroacetic acid (9%, final concentration) for 10 min on ice. The precipitates were filtered using Whatman GF/C glass microfiber filters that were preblocked in lysis buffer containing 2% milk. The filters were air dried overnight and bound radioactivity determined by scintillation counting.

Western blot analysis

Equal protein amounts (50 μg) were resolved by SDS-PAGE, transferred to nitrocellulose membranes, and immunoblotted with antibodies described above. After incubation with secondary antibody conjugated to horseradish peroxidase, the bands were detected with the enhanced chemiluminescence system (Amersham Biosciences, Piscataway, NJ; RPN2106). Immunoblots were scanned and quantified using Scion Image software.

Measurements of cytosolic free Ca^{2+}

INS-1 cells were seeded onto glass coverslips 1 d before the experiment. The cells were treated as indicated in the Fig. 9 legend for 6 h before the calcium measurements were initiated. The cells were loaded in RPMI medium with 3 μg/ml fura-2-AM for 30 min at 37 C under 5% CO_2. The coverslip was then placed in a thermostated Leiden chamber holder on the stage of a microscope (IM-35; Carl Zeiss) equipped with a ×40, 0.75 numerical aperture UV-I objective. A filter wheel (Sutter Instruments, Novato, CA) was used to alternately position the two excitation filters (340 ± 10 and 380 ± 10 nm; Chroma Technologies Corp., Brattleboro, VT) in front of a mercury lamp. The excitation light was directed to the cells via a 400-nm dichroic mirror. The data were recorded every 5–20 sec by irradiating the cells for 600 msec (340 nm) and 200 msec (380 nm) at each of the excitation wavelengths followed by acquisition of a bright-field image using Nomarski optics. Image acquisition was controlled by Metafluor software V 6.3 (Universal Imaging Corp., West Chester, PA). The emitted light was directed onto a dual bandpass (515 and 660 nm) emission filter placed in front of an Orca ER camera (Hamamatsu Photonics, Hamamatsu City, Japan) set to bin pixels by 8. The bright-field image was continuously monitored by placing a second 620-nm dichroic mirror in the light path to direct the nearly infrared light to a CCD-72 video camera (Dage MTI, Michigan City, IN). After mounting, the cells were washed once with Ca^{2+}-containing solution (140 nM NaCl, 5 mM KCl, 1 mM $MgCl_2$, 10 mM glucose, 20 mM HEPES, 100 μM EGTA, and 1.1 mM $CaCl_2$, pH 7.4). After basal measurements were made, the cells were placed in Ca^{2+}-free solution (140 nM NaCl, 5 mM KCl, 1 mM $MgCl_2$,10 mM glucose, 20 mM HEPES, and 100 μM EGTA, pH 7.4), and the ER Ca^{2+} stores were assessed by addition of 1 μM TG. The ratio of fluorescence intensity (F), F_{340nm}/F_{380nm}, for each cell was then normalized to the maximum determined in each individual measurement by treatment with 10 μM ionomycin in Ca^{2+}-containing solution.

Data analysis

Results are presented as mean ± SE. Statistical significance between two conditions was analyzed by the Student's paired *t* test and between several groups using one-way ANOVA, where $P < 0.05$ was considered statistically significant.

Results

Chronic FFA treatment induces β-cell apoptosis

FFA have been shown to induce apoptosis in pancreatic β-cell lines as well as in primary cultured β-cells (9–12, 14, 16, 27). In cultured cells and isolated islets, FFA treatments have been performed in both the presence and absence of serum. Generally, in the presence of serum, a longer incubation time is needed to observe cytotoxic effects in normal β-cells. We chose to perform the FFA treatments under serum-free conditions because this experimental paradigm has been used previously and has been suggested to potentially mimic the situation in type 2 diabetes (12).

We initially examined the effect of FFA treatment on apoptotic cell death in INS-1 pancreatic β-cells (28). Using a commercial kit that measures cytoplasmic histone-associated DNA fragments, a hallmark of apoptotic cells (29), little if any apoptosis was observed in control cells grown in the presence of serum. Treatment of the cells in serum-free conditions

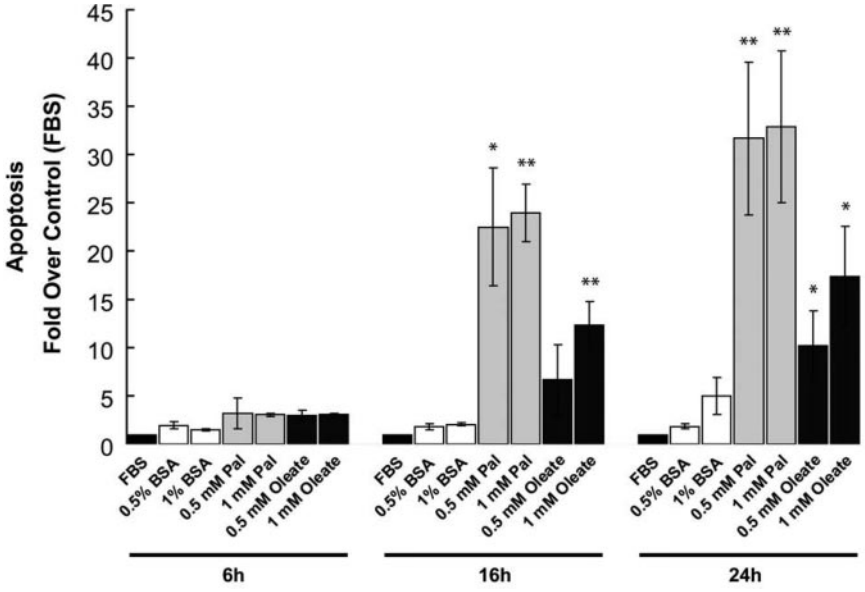

FIG. 1. Exposure of INS-1 pancreatic cells to palmitate and oleate induces β-cell apoptosis. INS-1 cells were treated with 0.5% BSA, 1% BSA, 0.5 mM palmitate/0.5% BSA, 1 mM palmitate/1% BSA, 0.5 mM oleate/0.5% BSA, or 1 mM oleate/1% BSA in media without serum for the times indicated on the x-axis. The cells were washed and subjected to lysis as described in *Materials and Methods*. Apoptosis was assessed using the cell death apoptosis kit (Roche) that measures the amount of cytoplasmic DNA-associated histone complexes. The levels of these complexes were slightly above background in cells grown in the presence of serum (+FBS), and consequently the values in all other conditions were normalized to cells grown in serum for each time point. Shown are the mean ± SE of three to five independent experiments with each condition performed in duplicate. *, $P < 0.05$; **, $P < 0.01$ *vs.* control (BSA).

resulted in a small increase in the amount of apoptotic cells after 24 h (Fig. 1; BSA). Significant apoptosis above BSA-treated controls was apparent after 24 h of treatment with 0.5 mM oleate and after 16–24 h of treatment with 1.0 mM oleate or palmitate ($P < 0.05$; Fig. 1). There was no difference in the extent of apoptosis induction by 0.5 mM compared with 1.0 mM palmitate, whereas 0.5 mM oleate tended to induce less β-cell apoptosis than 1.0 mM oleate. Consistent with previous findings, palmitate was more toxic to β-cells than oleate (10, 16). We also assayed the medium of FFA-treated INS-1 cells for histone-associated DNA fragments. This measures cell necrosis, which is characterized by disruption of the plasma membrane and leakage of cell contents. We noticed that palmitate treatment at both 0.5 and 1.0 mM caused increased levels of histone-associated DNA fragments, whereas oleate had no significant effect ($P < 0.05$) (supplemental Fig. 1, published as supplemental data on The Endocrine Society's Journals Online web site at http://endo.endojournals.org). Our results are consistent with reported findings showing that chronic oleate treatment causes little or no necrosis (10, 27, 30), whereas palmitate at 0.5 mM induces significant pancreatic β-cell necrosis (10, 30).

Palmitate but not oleate induces UPR signaling pathways

To determine whether FFA-induced β-cell death occurs as a result of ER stress, we examined whether FFA treatment can activate ER stress pathway signaling. ER stress activates three signal transduction cascades that emanate from the ER: the PERK, inositol-requiring enzyme 1 (IRE1), and ATF6 pathways (reviewed in Refs. 19 and 20). The PERK pathway is activated by autophosphorylation of the PERK kinase after ER stress (31). As shown in Fig. 2, *top*, treatment of β-cells with thapsigargin, a sarcoplasmic or endoplasmic reticulum calcium ATPase Ca^{2+}-ATPase blocker that depletes ER Ca^{2+} stores and is known to cause ER stress, caused the appearance of phosphorylated PERK. Interestingly, chronic treatment with 1.0 mM palmitate, but not oleate, also resulted in the appearance of phosphorylated PERK. Once activated, the PERK kinase phosphorylates the protein eIF2α (31). Phosphorylated eIF2α attenuates general protein translation but, in addition, selectively activates the translation of the ATF4 transcription factor mRNA (32). Palmitate but not oleate treatment increased nuclear ATF4 protein levels (Fig. 2, *bottom*), although both FFA increased the levels of phosphorylated eIF2α by 3 h of treatment (Fig. 3, A–C). However, only the palmitate-induced increase was significant based on band density analysis ($P < 0.05$; Fig. 3C). We also noticed that cells grown in the absence of serum for 16–24 h had elevated levels of phosphorylated eIF2α compared with control cells grown in serum.

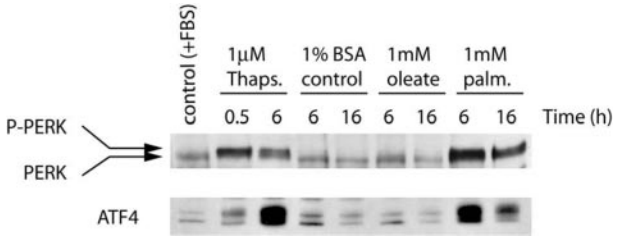

FIG. 2. Palmitate but not oleate induces PERK kinase phosphorylation and ATF4 activation. INS-1 cells were treated with 1% BSA (control), 1 mM oleate/1% BSA, 1 mM palmitate/1% BSA, or 1 μM thapsigargin (Thaps.) for the indicated times. After the treatments, either whole-cell lysates or nuclear extracts were prepared (see *Materials and Methods*). Whole-cell lysate fractions were immunoblotted using an anti-phospho-PERK antiserum (*top*), and the nuclear fractions were immunoblotted using an ATF4-specific antiserum (*bottom*).

The second ER stress pathway monitored was the IRE1 signaling pathway. IRE1, when activated, results in increased levels of the transcription factor XBP-1 (33, 34). Palmitate-treated cells had elevated XBP-1 protein levels by 6 h of treatment, an effect not observed with oleate treatment (Fig. 3, A and B). We also tested the effect of 0.5 mM palmitate on UPR pathway activation and observed similar results to that obtained with 1.0 mM palmitate (supplemental Fig. 2).

Upon activation, both of these UPR signaling pathways lead to elevated transcription and subsequent translation of several classes of genes, including the major ER chaperone proteins such as Grp78/BiP (19, 20). Interestingly, however, the steady-state protein levels of none of the major ER chaperones tested (Grp78/BiP, Grp94, and PDI) was altered by either chronic oleate or palmitate treatment (Fig. 3). As a positive control, treatment with tunicamycin, a commonly used pharmacological ER stress inducer, caused increased steady-state protein levels of both Grp78 and Grp94 (Fig. 3).

In the face of persistent ER stress, the PERK and IRE1 signaling pathways induce transcription and translation of proapoptotic factors such as the protein CHOP/GADD153 (35). By 6 h of treatment with 1 mM palmitate, CHOP protein levels were significantly elevated, an effect not observed with oleate treatment ($P < 0.05$; Fig. 3D). Palmitate at 0.5 mM induced a similar increase in CHOP protein levels (supplemental Fig. 2B). Apart from inducing slightly the phosphorylation of eIF2α, oleate did not appear to elicit UPR signaling pathways in INS-1 cells even at high (1 mM) concentrations.

Chaperone protein levels are not increased by FFA treatment

Despite clearly activating the UPR signaling pathways, palmitate treatment did not elevate steady-state ER chaperone protein levels (Fig. 3, E and F, and supplemental Fig. 2). This was surprising given the known effects of UPR pathway signaling leading to induction of ER chaperones (19, 20) and the fact that a recent study has reported that FFA augment Grp78 mRNA by about 2-fold (16). To test whether FFA affect Grp78 translation, we examined the rate of [^{35}S]methionine incorporation into newly synthesized Grp78 in the presence and absence of FFA. Although tunicamycin clearly enhanced [^{35}S]methionine incorporation into newly synthesized Grp78, neither palmitate nor oleate had any effect (Fig. 4). Thus, palmitate-activated UPR signaling, as opposed to pharmacological induction of UPR signaling, does not lead to induction of chaperone protein levels.

Palmitate alters the ER morphology in INS-1 β-cells

We also examined the localization of the ER chaperone proteins in control and FFA-treated INS-1 cells by immunofluorescence microscopy using an antibody recognizing the KDEL sequence. Control cells had a typical reticular ER

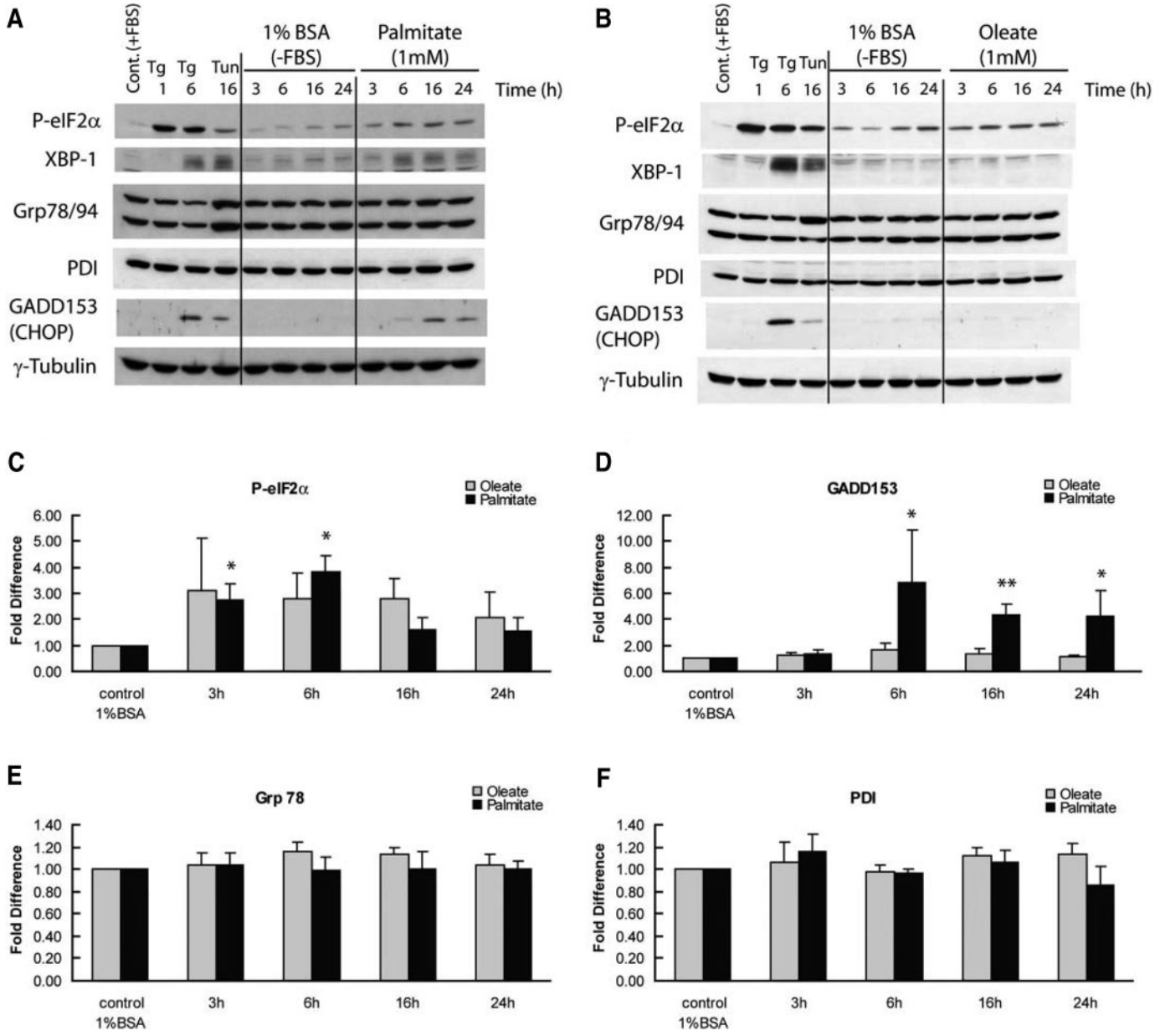

FIG. 3. Induction of ER stress markers after FFA treatments. Representative Western blots are shown after the treatments with 1 mM palmitate/1% BSA (A) and 1 mM oleate/1% BSA (B). INS-1 cells were treated with 1% BSA or 1 mM FFA/1% BSA in the absence of serum for the indicated times as described in *Materials and Methods*. Thapsigargin (Tg) and tunicamycin (Tun) were used as positive controls for ER stress induction relative to control cells grown in the presence of serum [Cont. (+FBS)]. After the treatment, the cells were lysed and immunoblotted using anti-phospho-eIF2α, XBP-1, Grp78/94, PDI, GADD153/CHOP, and tubulin antibodies. Western blots were scanned and quantified using Scion Image software. All values were normalized to a loading control (tubulin). C–F, Fold induction was determined as a ratio of FFA-treated over BSA-treated values at the same time point. An average of at least three independent experiments is shown (±SE). *, $P < 0.05$; **, $P < 0.01$ *vs.* control.

staining pattern throughout the cell (Fig. 5B). However, exposure of the cells for 6 h to palmitate, but not oleate, altered the fluorescence distribution. The KDEL signal in palmitate-treated cells appeared in large bright punctate/aggregate structures, both close to the nucleus and near the cell periphery (Fig. 5E). There were also areas in the cell (in addition to the nucleus) that were completely devoid of labeling. This punctate/aggregate distribution was also observed in cells treated with thapsigargin, although the labeling appeared throughout the cell (Fig. 5F). Comparable results were obtained using an antibody specific for Grp78. A similar KDEL and Grp78 localization was observed after treatment of INS-1 cells with 0.5 mM palmitate/0.5% BSA (results not shown).

The morphology of the palmitate-treated cells at the light microscopy level was also abnormal as the cells appeared condensed and angular (Fig. 6 *bottom right*). These morphological changes were not elicited by oleate treatment (Fig. 6, *middle right*). Because the localization of ER chaperones and

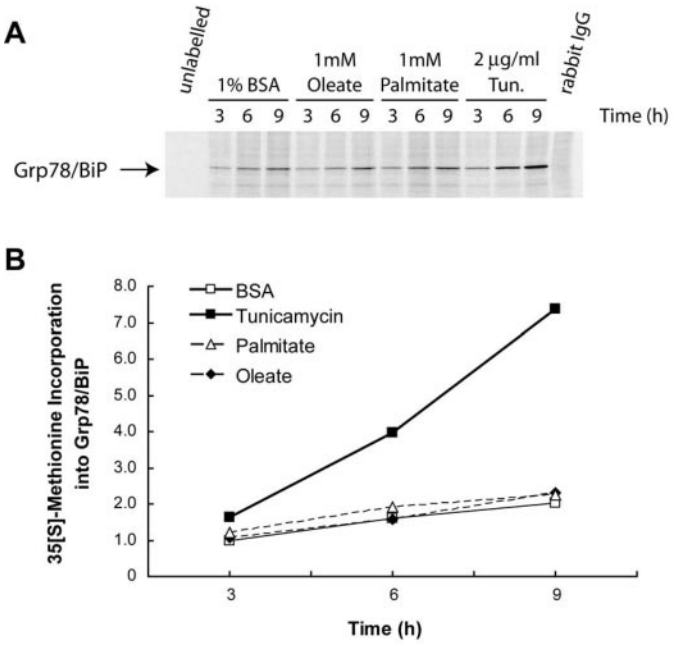

FIG. 4. Treatment of INS-1 cells with FFA does not induce increased translation of Grp78/BiP. A, INS-1 cells were treated with 1% BSA, 1 mM oleate/1% BSA, 1 mM palmitate/1% BSA, and 2 μg/ml tunicamycin in the presence of [^{35}S]L-methionine. After the indicated time points, the cells were lysed and immunoprecipitated using rabbit polyclonal BiP antiserum as described in *Materials and Methods*. A nonspecific rabbit IgG antiserum was used to immunoprecipitate the [^{35}S]methionine-labeled BSA sample as a negative control (last lane). The immunoprecipitates were resolved on SDS-PAGE, and the gel was dried and exposed to a phosphorimager screen. B, Quantitation of band intensity was done using ImageQuant software (Molecular Dynamics). To determine the rate of [^{35}S]methionine incorporation over time, the values were normalized to 1% BSA (3-h time point). Plotted are the average results from two independent experiments.

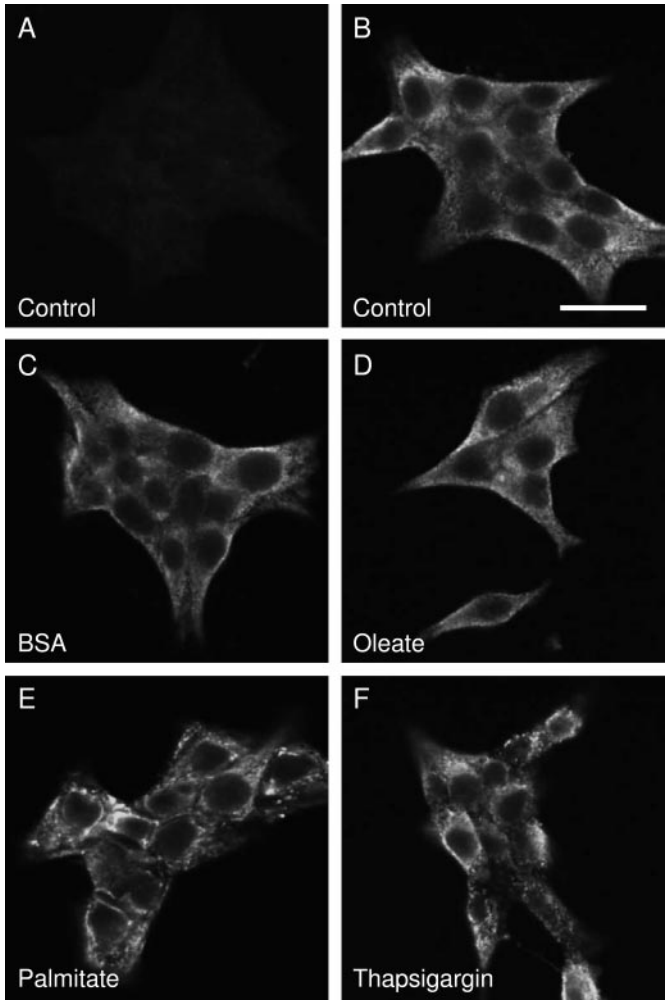

FIG. 5. Altered distribution of KDEL sequence-containing proteins in cells exposed to palmitate but not oleate. INS-1 cells were left untreated (control, B) or treated with 1% BSA (C), 1 mM oleate/1% BSA (D), 1 mM palmitate/1% BSA (E), or 1 μM thapsigargin (F) for 6 h. After the treatments, the cells were washed in PBS, fixed, and immunostained with an anti-KDEL antibody. A, Control of cells labeled with secondary antibody only. *Bar*, 20 μm.

Grp78 was markedly altered by palmitate (Fig. 5), we examined the effect of palmitate on a transmembrane ER protein. We transiently transfected INS-1 cells with the ER targeted transmembrane protein ATF6 (tagged with an HA epitope) (36). The protein had a typical reticular staining pattern in control and oleate-treated cells (Fig. 6, *top* and *middle*). However, in palmitate-treated cells, the distribution of the fusion construct was markedly altered. The HA-ATF6 protein was distributed around the nucleus and periphery of the cell, and there were large areas within the cell completely devoid of the protein (Fig. 6, *bottom left*).

Our results at the light microscopy level suggested that palmitate was altering ER morphology. Indeed, by electron microscopy, we observed a markedly altered cell morphology in palmitate-treated INS-1 cells by as little as 30 min of treatment (Fig. 7, A compared with B). In palmitate-treated cells, we observed electron-lucent clefts extending throughout the cytoplasm. In many places, no limiting membrane was visible in these clefts, but in some cases they were clearly in continuity with the lumen of the ER, suggesting that they arose from an altered ER (Fig. 7C). The ER chaperone Grp78 is localized along the inner area of the electron-lucent structures, supporting the fact that these structures are continuous with the ER (Fig. 7D). Interestingly, we observed very limited alterations of the nuclear envelope in these cells despite the continuity of the nuclear envelope with the ER. These results are similar to a very recent study showing that the ER morphology in INS-1 cells treated with palmitate for 24 h was severely dilated, apparently because of the accumulation of tripalmitin in the ER (37). In addition, we observed altered mitochondrial and Golgi morphology in palmitate-treated cells (Fig. 7, E and F). Similar morphological changes were observed with 0.5 mM palmitate (supplemental Fig. 3).

Palmitate does not enhance translation or significantly alter ER Ca^{2+} homeostasis

As shown above, chronic palmitate treatment activates UPR signaling pathways. UPR signaling is initiated by increased demand for protein-folding capacity, which titrates ER chaperones away from the luminal domains of ER stress-sensing proteins, causing their activation (38, 39). This can occur if misfolded proteins accumulate during pathophysiological conditions or by enhanced translation that may oc-

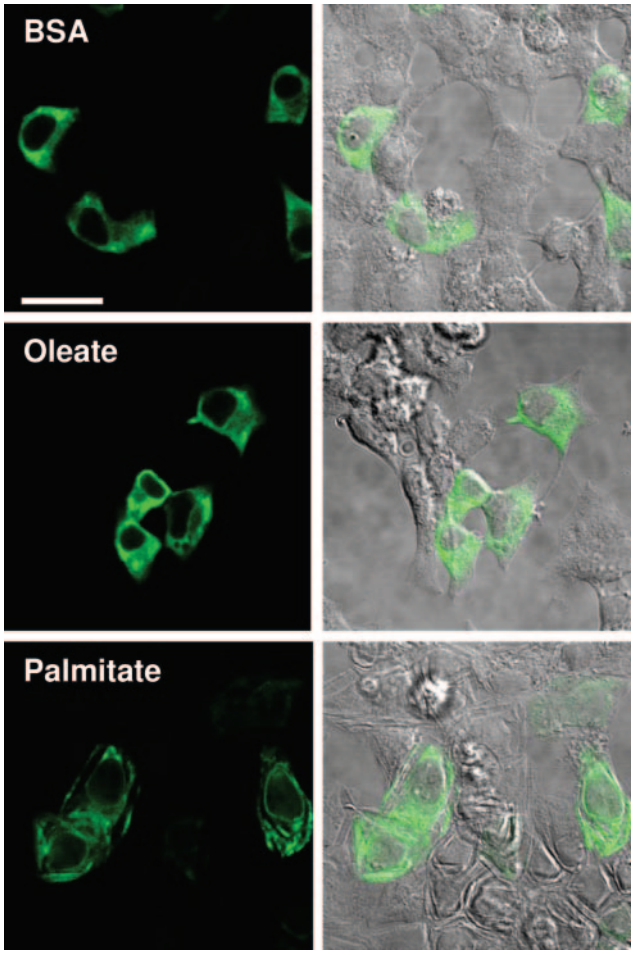

FIG. 6. Effect of palmitate and oleate on HA-ATF6 distribution in INS-1 cells. INS-1 cells were transiently transfected with HA-ATF6. Twenty-four hours after transfection, the cells were treated for 6 h with 1% BSA, 1 mM oleate/1% BSA, or 1 mM palmitate/1% BSA for 6 h. The cells were then fixed and immunostained with anti-HA. Shown are representative confocal images of HA immunostaining (*left*) and the merged fluorescence and differential interference contrast images of the cells (*right*). *Bar*, 20 μm.

cur physiologically, such as in glucose-stimulated β-cells (22). Thus, it is possible that palmitate enhances translation acutely, leading to an increase in ER client protein load and consequently activation of UPR pathways. As shown in Fig. 8, however, treatment with oleate or palmitate for 3–9 h actually causes a small reduction in general translation rate as measured by incorporation of radiolabeled leucine into total cellular protein, although this was not significant. This is consistent with the increased levels of phosphorylated eIF2α after FFA treatment (Fig. 3).

Because translation rates are not enhanced by FFA, even at early time points after treatment, it is possible that palmitate gradually causes the accumulation of misfolded proteins in the ER. Accumulation of misfolded proteins can occur when the ER luminal environment is perturbed. One such perturbation could be depletion of ER Ca^{2+} levels. We therefore examined the effect of FFA on cytoplasmic Ca^{2+} levels in pancreatic INS-1 cells. Cytoplasmic calcium levels can be monitored by the membrane-permeant calcium indicator fura-2-AM (40). Cells can subsequently be exposed to thapsigargin, which dissipates ER calcium stores resulting in increased cytosolic calcium that indirectly reflects ER Ca^{2+} levels (41). Palmitate or oleate-treated cells had a similar cytoplasmic calcium increase after thapsigargin addition as BSA-treated controls, indicating that FFA treatment does not significantly alter ER Ca^{2+} concentrations (Fig. 9). Therefore, alteration in ER Ca^{2+} homeostasis is unlikely to be the underlying mechanism of how palmitate induces ER stress.

Discussion

Obesity is a major risk factor for the development of type 2 diabetes. Chronically elevated FFA may contribute to the progression of this disease by promoting pancreatic β-cell death (5–8). Consistent with previous observations (9–12, 14, 16, 27), chronic (16–24 h) treatment of pancreatic β-cells with palmitate or oleate induces considerable β-cell apoptosis (Fig. 1). In this study, the FFA treatment was performed under serum-free conditions, where both palmitate and oleate have been shown to markedly enhance apoptosis (12), possibly as a result of the lack of leptin, a hormone with lipotoxicity-protective properties (42). Thus, serum-free conditions may mimic in a cellular context both the oxidative stress situation that occurs in type 2 diabetes (12) as well as leptin resistance that may contribute to lipotoxicity in diet-induced obesity (8). In addition, our studies were performed in media containing 11.1 mM glucose, which is higher than basal levels (3–5 mM) and may contribute to the cytotoxic effects we observed.

The recent finding that obesity is associated with cellular ER stress in several tissues (18) suggests that ER stress could play a role in FFA-induced β-cell death. Cellular ER stress activates three distinct signaling pathways that are initiated by stress-sensing proteins located in the ER membrane. The PERK, IRE1, and ATF6 signaling pathways have been extensively characterized (19, 20). Collectively, these UPR signaling pathways initiate cell-protective mechanisms that attempt to restore ER protein-folding capacity by transiently inhibiting translation (PERK pathway) and inducing a variety of gene products that either enhance protein folding capacity (ER chaperone proteins) or degrade terminally misfolded or aggregated proteins (ER-associated degradation system). In the face of persistent ER stress, however, apoptotic pathways are initiated. The CHOP/GADD153 transcription factor (35), caspases (43), and c-Jun N-terminal kinase (44, 45) have been implicated in this aspect of the UPR, although the downstream pathways are only beginning to be characterized (46, 47).

Here we report that although both of the FFA induced β-cell apoptosis, only palmitate activated the PERK and IRE1 pathways of the UPR (measured by phospho-PERK, ATF4, and XBP-1 protein levels). Furthermore, palmitate, but not oleate, up-regulated the levels of the CHOP transcription factor, which in part mediates ER stress-induced cell death (35). What is particularly striking is the fact that although palmitate clearly activates PERK and IRE1 signaling, the main ER chaperone target genes of these signaling pathways are not induced by palmitate (19). Thus, it appears that the beneficial aspects of UPR induction are bypassed and the

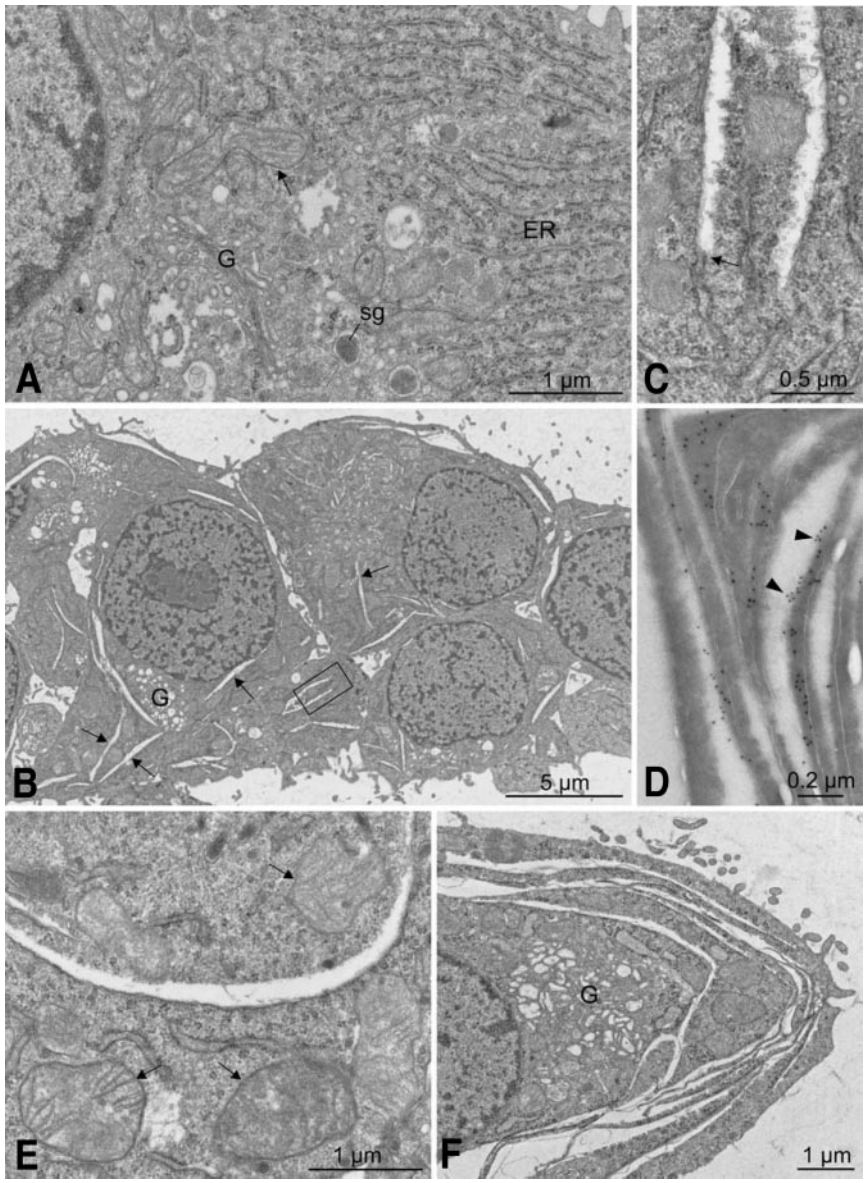

FIG. 7. Effect of palmitate on the morphology of INS-1 cells. INS-1 cells untreated or treated with 1 mM palmitate/1% BSA were examined by electron microscopy. A, Untreated INS-1 cells show the familiar appearance of rough ER (ER), Golgi complex (G), mitochondria (*arrow*), and secretory granules (sg). B, After 30 min of treatment with 1 mM palmitate/1% BSA, INS-1 cells contain electron-lucent clefts (*arrows*) extending throughout the cytoplasm and vacuolar Golgi complex. The *arrow* in the *boxed area* enlarged in C shows the continuity of a cleft with an apparently unaltered ER cisterna. D, Immunogold labeling with antibodies to the ER chaperone protein Grp78/BiP shows *gold particles* lining the edge of the clefts (*arrowheads*). E, Compared with the control (*arrow* in A), palmitate-treated INS-1 cells contain swollen mitochondria (*arrows*). F, After 3 h of incubation with palmitate, one observes an extensive increase in the size and number of clefts.

destructive aspects (CHOP induction) are induced by this fatty acid.

The fact that palmitate does not up-regulate Grp78 expression is somewhat surprising because the IRE1/XBP-1 pathway signaling has been described to be involved in inducing transcription of ER chaperone genes such as Grp78 (34). However, the ATF6 signaling pathway of the UPR has also been implicated in inducing chaperone expression (19, 48). Furthermore, ATF6 can induce Grp78 transcription in the absence of XBP-1 and appears to be the predominant pathway for Grp78 induction (49). Thus, it is possible that palmitate does not activate the ATF6 pathway in INS-1 cells. Whether palmitate can induce the ATF6 pathway remains to be tested. A recent report has shown that FFA can activate a luciferase-based ATF6 promoter construct transfected into INS-1 cells (16). However, this is not evidence that the ATF6 pathway is activated because activation of ATF6 involves its translocation from the ER to the Golgi, where it undergoes proteolysis releasing the cytosolic transcriptional activation domain (50).

Our results differ somewhat from Kharroubi *et al.* (16), who recently reported, based on real-time RT-PCR analysis, that both oleate and palmitate increased the mRNA levels of ATF4 (~50%) and BiP (~2-fold) after 24 h of treatment. However, the protein levels of these gene products were not measured in that study. Furthermore, several microarray studies have failed to detect increases in mRNA abundance of common ER chaperones in response to FFA treatment (51–53). Thus, it is unlikely that FFA elevate Grp78 protein levels to a significant degree. Our results show that palmitate is unable to induce Grp78 expression, and as a consequence, the β-cell is deprived of one of the main survival mechanisms during ER stress.

How does palmitate induce ER stress? Palmitate does not enhance protein synthesis; thus, it is not increasing ER client protein load. Our results suggest that palmitate might alter the

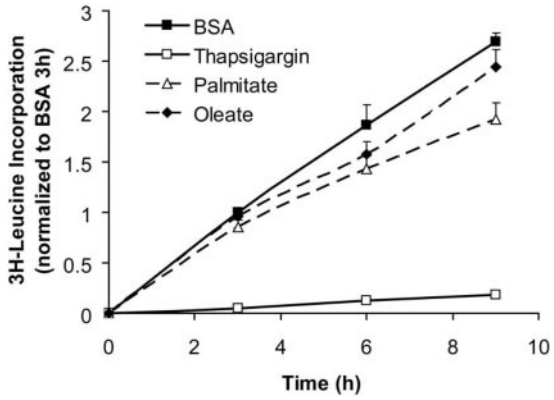

FIG. 8. Effect of FFA on the incorporation of [^{3}H]leucine into total cellular protein. INS-1 cells were labeled with [^{3}H]leucine in the presence of 1% BSA, 1 mM palmitate/1% BSA, 1 mM oleate/1% BSA, or 1 μM thapsigargin for various times. Total protein was trichloroacetic acid precipitated and [^{3}H]leucine incorporation measured by scintillation counting. [^{3}H]Leucine incorporation is normalized to the BSA 3-h treatment, and the mean incorporation from three independent experiments is shown.

ER environment and as a consequence cause the production of misfolded proteins. Although we have no direct evidence for this, palmitate does significantly alter the distribution of the major ER chaperone Grp78 from a normally reticular ER localization pattern to a largely punctate/aggregated distribution, similar to the effect caused by thapsigargin. Furthermore, a similar abnormal distribution of Grp78 has been observed in cells treated with proteasome inhibitors, which prevent ER-associated degradation (54). Finally, a recent study in a mouse model of diabetes has shown that newly synthesized proinsulin is bound to Grp78 and accumulates in the ER of mouse β-cells exposed to high-fat feeding (55).

The drastic palmitate-induced ER morphological perturbation that we observed was reported during the course of our studies (37). This report observed that after 24 h of palmitate exposure, INS-1 cells accumulated insoluble tripalmitin triglyceride within the ER that likely causes the gross ER morphology observed (37). Here we also show that ER morphology is altered after only a short palmitate exposure of 30 min, although it takes significantly longer (~6 h) before ER stress pathways are activated.

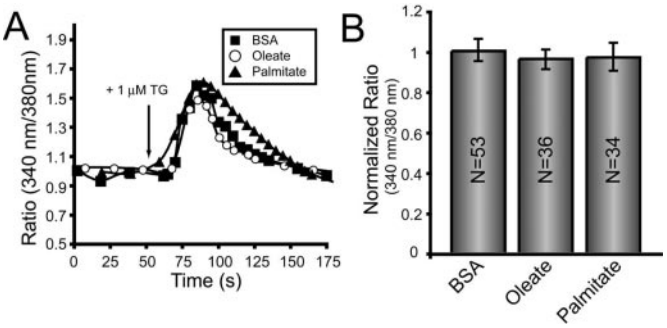

FIG. 9. Effect of oleate and palmitate on ER Ca^{2+} stores. INS-1 cells were pretreated with 1% BSA, 1 mM oleate/1% BSA, or 1 mM palmitate/1% BSA for 6 h before loading with 3 μg/ml fura-2-AM for 30 min, washed, and placed in a Ca^{2+}-free medium. Cytosolic free Ca^{2+} concentration was measured as described in *Materials and Methods*. Where indicated, 1 μM thapsigargin (TG) was added to deplete the ER Ca^{2+} stores. A, Representative experiments illustrating the fluorescence ratio of a BSA-treated cell (■), oleate-treated cell (○), and a palmitate-treated cell (▲). B, Summary of the effects BSA, oleate, and palmitate on Ca^{2+} concentration. The fluorescence ratio attained after addition of TG in calcium-free medium is presented. The data are the means ± SD of the number of cells indicated from four independent experiments.

It is possible that the tripalmitin accumulation in the ER alters the protein-folding environment, increasing the amount of misfolded protein, which in turn activates the UPR. There are several possible ER perturbations that would decrease protein-folding capacity, such as depletion of ER Ca^{2+} levels, inhibition of normal glycosylation, or alterations in ER redox state. It is unlikely that alterations in ER Ca^{2+} have a major role because no significant effect was observed in ER releasable Ca^{2+} stores in FFA-treated cells. The means by which palmitate affects ER homeostasis that ultimately leads to ER stress induction requires additional study.

Although not as potent as palmitate, oleate is also cytotoxic to β-cells. In this study, we show that ER stress induction does not appear to be a major contributor to oleate-induced β-cell death. As mentioned in the introductory section, both oleate- and palmitate-induced pancreatic β-cell death can also be initiated by additional mechanisms (9, 12, 14, 17). The fact that palmitate also significantly induces ER stress in β-cells may explain the higher cytotoxic potential of this fatty acid (10, 16).

In summary, we have shown that palmitate but not oleate induces significant ER stress contributing to INS-1 pancreatic β-cell apoptosis. Future studies are required to determine the nature of the ER perturbations elicited by palmitate to ultimately cause ER stress as well as the molecular basis behind the lack of chaperone (Grp78) induction after palmitate-induced ER stress. Finally, oleate in combination with palmitate has been shown to prevent to some degree the deleterious effects of palmitate (56). It will be interesting to determine whether oleate can protect against palmitate-induced ER stress.

Acknowledgments

We thank Dr. Bernardo Yusta for help with some of the Western blots, Dr. Ron Prywes (Columbia University, New York, NY) for the HA-ATF6 construct, and Dr. Ingrid Haas for the polyclonal anti-Grp78 antibody. We thank Drs. Bernardo Yusta, Roger Unger, Amira Klip, and Sergio Grinstein for helpful comments on the manuscript.

Received November 23, 2005. Accepted March 24, 2006.

Address all correspondence and requests for reprints to: Allen Volchuk, Division of Cell and Molecular Biology, Toronto General Research Institute, University Health Network, 200 Elizabeth Street, MBRC 4R402 Toronto, Ontario, Canada M5G 2C4. E-mail: avolchuk@uhnres.utoronto.ca.

T.T. was supported in part by a Banting and Best Diabetes Centre (University of Toronto) summer studentship award. This work was supported by grants to A.V. from The Canadian Institutes of Health Research and The Banting Research Foundation and by start-up funds from the University Health Network, Toronto, Canada. Infrastructure support for the A.V. laboratory was provided by funding from the Canadian Foundation for Innovation and the Ontario Innovation Trust. We thank the Pôle Facultaire de Microscopie Ultrastructurale at the University of Geneva Medical School for access to electron microscopy equipment. A.V. is the recipient of a Tier II Canada Research Chair award.

Disclosures: The authors have no financial conflict of interest.

References

1. **Poitout V, Robertson RP** 1996 An integrated view of β-cell dysfunction in type-II diabetes. Annu Rev Med 47:69–83
2. **Ahren B** 2005 Type 2 diabetes, insulin secretion and β-cell mass. Curr Mol Med 5:275–286

3. **Eizirik DL, Mandrup-Poulsen T** 2001 A choice of death: the signal transduction of immune-mediated β-cell apoptosis. Diabetologia 44:2115–2133
4. **Wellen KE, Hotamisligil GS** 2005 Inflammation, stress and diabetes. J Clin Invest 115:1111–1119
5. **Haber EP, Ximenes HMA, Procopio J, Carvalho CRO, Curi R, Carpinelli AR** 2002 Pleiotropic effects of fatty acids on pancreatic β-cells. J Cell Physiol 194:1–12
6. **Robertson RP, Harmon J, Tran POT, Poitout V** 2004 β-Cell glucose toxicity, lipotoxicity, and chronic oxidative stress in type 2 diabetes. Diabetes 53:S119–S124
7. **Unger RH** 1995 Lipotoxicity in the pathogenesis of obesity-dependent NIDDM. Genetic and clinical implications. Diabetes 44:863–870
8. **Unger RH, Zhou Y-T** 2001 Lipotoxicity of β-cells in obesity and in other causes of fatty acid spillover. Diabetes 50:S118–S121
9. **Carlsson C, Borg LA, Welsh N** 1999 Sodium palmitate induces partial mitochondrial uncoupling and reactive oxygen species in rat pancreatic islets *in vitro*. Endocrinology 140:3422–3428
10. **Cnop M, Hannaert JC, Hoorens A, Eizirik DL, Pipeleers DG** 2001 Inverse relationship between cytotoxicity of free fatty acids in pancreatic islet cells and cellular triglyceride accumulation. Diabetes 50:1771–1777
11. **Maedler K, Spinas GA, Dyntar D, Moritz W, Kaiser N, Donath MY** 2001 Distinct effects of saturated and monounsaturated fatty acids on β-cell turnover and function. Diabetes 50:69–76
12. **Maestre I, Jordan J, Calvo S, Reig JA, Cena V, Soria B, Prentki M, Roche E** 2003 Mitochondrial dysfunction is involved in apoptosis induced by serum withdrawal and fatty acids in the β-cell line Ins-1. Endocrinology 144:335–345
13. **Shimabukuro M, Ohneda M, Lee Y, Unger RH** 1997 Role of nitric oxide in obesity-induced β cell disease. J Clin Invest 100:290–295
14. **Shimabukuro M, Zhou YT, Levi M, Unger RH** 1998 Fatty acid-induced β cell apoptosis: a link between obesity and diabetes. Proc Natl Acad Sci USA 95:2498–2502
15. **Unger RH, Orci L** 2002 Lipoapoptosis: its mechanism and its diseases. Biochim Biophys Acta 1585:202–212
16. **Kharroubi I, Ladriere L, Cardozo AK, Dogusan Z, Cnop M, Eizirik DL** 2004 Free fatty acids and cytokines induce pancreatic β-cell apoptosis by different mechanisms: role of nuclear factor-κB and endoplasmic reticulum stress. Endocrinology 145:5087–5096
17. **Piro S, Anello M, Di Pietro C, Lizzio MN, Patane G, Rabuazzo AM, Vigneri R, Purrello M, Purello F** 2002 Chronic exposure to free fatty acids or high glucose induces apoptosis in rat pancreatic islets: possible role of oxidative stress. Metabolism 51:1340–1347
18. **Ozcan U, Cao Q, Yilmaz E, Lee AH, Iwakoshi NN, Ozdelen E, Tuncman G, Gorgun C, Glimcher LH, Hotamisligil GS** 2004 Endoplasmic reticulum stress links obesity, insulin action and type 2 diabetes. Science 306:457–461
19. **Harding HP, Calfon M, Urano F, Novoa I, Ron D** 2002 Transcriptional and translational control in the mammalian unfolded protein response. Annu Rev Cell Dev Biol 18:575–599
20. **Zhang K, Kaufman RJ** 2004 Signaling the unfolded protein response from the endoplasmic reticulum. J Biol Chem 279:25935–25938
21. **Araki E, Oyadomari S, Mori M** 2003 Impact of endoplasmic reticulum stress pathway on pancreatic β-cells and diabetes mellitus. Exp Biol Med 228:1213–1217
22. **Harding HP, Ron D** 2002 Endoplasmic reticulum stress and the development of diabetes. Diabetes 51:S455–S461
23. **Cousin SP, Hugl SR, Wrede CE, Kajio H, Myers MG, Rhodes CJ** 2001 Free fatty acid-induced inhibition of glucose and insulin-like growth factor 1-induced deoxyribonucleic acid synthesis in the pancreatic β-cell line INS-1. Endocrinology 142:229–240
24. **Tandler B** 1990 Improved uranyl acetate staining for electron microscopy. J Electron Microsc Tech 16:81–82
25. **Volchuk A, Amherdt M, Ravazzola M, Brugger B, Rivera VM, Clackson T, Perrelet A, Sollner TH, Rothman JE, Orci L** 2000 Megavesicles implicated in the rapid transport of intracisternal aggregates across the Golgi stack. Cell 102:335–348
26. **Liou W, Geuze H, Slot JW** 1996 Improving structural integrity of cryosections for immunogold labeling. Histchem Cell Biol 106:41–58
27. **Wrede CE, Dickson LM, Lingohr MK, Briaud I, Rhodes CJ** 2002 Protein kinase B/Akt prevents fatty acid-induced apoptosis in pancreatic β-cells (INS-1). J Biol Chem 277:49676–49684
28. **Asfari M, Janjic D, Meda P, Li G, Halban PA, Wollheim CB** 1992 Establishment of 2-mercaptoethanol-dependent differentiated insulin-secreting cell lines. Endocrinology 130:167–178
29. **Saraste A, Pulkki K** 2000 Morphologic and biochemical hallmarks of apoptosis. Cardiovasc Res 45:528–537
30. **Cnop M, Hannaert JC, Pipeleers DG** 2002 Troglitazone does not protect rat pancreatic β-cells against free fatty acid-induced cytotoxicity. Biochem Pharmacol 63:1281–1285
31. **Harding HP, Zhang Y, Ron D** 1999 Protein translation and folding are coupled by an endoplasmic reticulum-resident kinase. Nature 397:271–274
32. **Harding HP, Novoa I, Zhang Y, Zeng H, Wek R, Schapira M, Ron D** 2000 Regulated translation initiation controls stress-induced gene expression in mammalian cells. Mol. Cell 6:1099–1108
33. **Calfon M, Zeng H, Urano F, Till JH, Hubbard SR, Harding HP, Clark SG, Ron D** 2002 IRE1 couples endoplasmic reticulum load to secretory capacity by processing the XBP-1 mRNA. Nature 415:92–96
34. **Yoshida H, Matsui T, Yamamoto A, Okada T, Mori K** 2001 XBP1 mRNA is induced by ATF6 and spliced by IRE1 in response to ER stress to produce a highly active transcription factor. Cell 107:881–891
35. **Oyadomari S, Mori M** 2004 Roles of CHOP/GADD153 in endoplasmic reticulum stress. Cell Death Differ 11:381–389
36. **Chen X, Shen J, Prywes R** 2002 The luminal domain of ATF6 senses endoplasmic reticulum (ER) stress and causes translocation of ATF6 from the ER to the Golgi. J Biol Chem 277:13045–13052
37. **Moffitt JH, Fielding BA, Evershed R, Berstan R, Currie JM, Clark A** 2005 Adverse physicochemical properties of tripalmitin in β cells lead to morphological changes and lipotoxicity in vitro. Diabetologia 48:1819–1829
38. **Bertolotti A, Zeng Y, Hendershot LM, Harding HP, Ron D** 2000 Dynamic interaction of BiP and ER stress transducers in the unfolded-protein response. Nat Cell Biol 2:326–332
39. **Shen J, Chen X, Hendershot L, Prywes R** 2002 ER stress regulation of ATF6 localization by dissociation of Bip/GRP78 binding and unmasking of Golgi localization signals. Dev Cell 3:99–111
40. **Tsien RY, Rink TJ, Poenie M** 1985 Measurement of cytoplasmic free Ca^{2+} in individual small cells using fluorescence microscopy with dual excitation wavelengths. Cell Calcium 6:145–157
41. **Lytton J, Westlin M, Hanley MR** 1991 Thapsigargin inhibits the sarcoplasmic reticulum Ca-ATPase family of calcium pumps. J Biol Chem 266:17067–17071
42. **Unger RH, Zhou YT, Orci L** 1999 Regulation of fatty acid homeostasis in cells: novel role of leptin. Proc Natl Acad Sci USA 96:2327–2332
43. **Momoi T** 2004 Caspases involved in ER stress-mediated cell death. J Chem Neuroanat 28:101–105
44. **Kadowaki H, Nishitoh H, Ichijo H** 2004 Survival and apoptosis signals in ER stress: the role of protein kinases. J Chem Neuroanat 28:93–100
45. **Urano F, Wang X, Bertolotti A, Zhang Y, Chung P, Harding HP, Ron D** 2000 Coupling of stress in the ER to activation of JNK protein kinases by transmembrane protein kinase IRE1. Science 287:664–666
46. **Marciniak SJ, Yun CY, Oyadomari S, Novoa I, Zhang Y, Jungries R, Nagata K, Harding HP, Ron D** 2004 CHOP induces death by promoting protein synthesis and oxidation in the stressed endoplasmic reticulum. Genes Dev 18:3066–3077
47. **Srinivasan S, Ohsugi M, Liu Z, Fatrai S, Bernal-Mizrachi E, Permutt MA** 2005 Endoplasmic reticulum stress-induced apoptosis is partly mediated by reduced insulin signaling through phosphatidylinositol 3-kinase/Akt and increased glycogen synthase kinase-3β in mouse insulinoma cells. Diabetes 54:968–975
48. **Li M, Baumeister P, Roy B, Phan T, Foti D, Luo S, Lee AS** 2000 ATF6 as a transcription activator of the endoplasmic reticulum stress element: thapsigargin stress-induced changes and synergistic interactions with NF-Y and YY1. Mol Cell Biol 20:5096–5106
49. **Yamamoto K, Yoshida H, Kokame K, Kaufman RJ, Mori K** 2004 Differential contributions of ATF6 and XBP1 to the activation of endoplasmic reticulum stress-responsive cis-acting elements ERSE, UPRE and ERSE-II. J Biochem 136:343–350
50. **Haze K, Yoshida H, Yanagi H, Yura T, Mori K** 1999 Mammalian transcription factor ATF6 is synthesized as a transmembrane protein and activated by proteolysis in response to endoplasmic reticulum stress. Mol Biol Cell 10: 3787–3799
51. **Busch AK, Cordery D, Denyer GS, Biden TJ** 2002 Expression profiling of palmitate and oleate-regulated genes provides novel insights into the effect of chronic lipid exposure on pancreatic β-cell function. Diabetes 51:977–987
52. **Wang X, Li H, De Leo D, Guo W, Koshkin V, Fantus IG, Giacca A, Chan CB, Der S, Wheeler MB** 2004 Gene and protein kinase expression profiling of reactive oxygen species-associated lipotoxicity in the pancreatic β-cell line MIN6. Diabetes 53:129–140
53. **Xiao J, Gregersen S, Kruhoffer M, Pedersen SB, Orntoft TF, Hermansen K** 2001 The effect of chronic exposure to fatty acids on gene expression in clonal insulin-producing cells: studies using high density oligonucleotide microarray. Endocrinology 142:4777–4784
54. **Kitiphongspattana K, Mathews CE, Leiter EH, Gaskins HR** 2005 Proteasome inhibition alters glucose-stimulated (pro)insulin secretion and turnover in pancreatic β-cells. J Biol Chem 280:15727–15734
55. **Scheuner D, Vander Mierde D, Song B, Flamez D, Creemers JWM, Tsukamoto K, Ribick M, Schuit FC, Kaufman RJ** 2005 Control of mRNA translation preserves endoplasmic reticulum function in β cells and maintains glucose homeostasis. Nature Med 11:757–764
56. **Maedler K, Oberholzer J, Bucher P, Spinas GA, Donath MY** 2003 Monounsaturated fatty acids prevent the deleterious effects of palmitate and high glucose on human pancreatic β-cell turnover and function. Diabetes 52:726–733

Endocrinology **is published monthly by The Endocrine Society (http://www.endo-society.org), the foremost professional society serving the endocrine community.**